1989

NASA/ASEE SUMMER FACULTY FELLOWSHIP PROGRAM

MARSHALL SPACE FLIGHT CENTER
THE UNIVERSITY OF ALABAMA IN HUNTSVILLE

INVESTIGATION OF SSME ALTERNATE HIGH PRESSURE FUEL TURBOPUMP LIFT-OFF SEAL FLUID AND STRUCTURAL DYNAMIC INTERACTION

Prepared by:	David A. Elrod
Academic Rank:	Assistant Professor
University and Department:	Virginia Polytechnic Institute and State University Mechanical Engineering

NASA/MSFC:
    Laboratory:
    Division:
    Branch:
	
	Propulsion
	Component Development
	Turbomachinery and Combustion Devices

MSFC Colleague:	Henry P. Stinson
Date:	July 28, 1989
Contract No.:	The University of Alabama in Huntsville NGT-01-008-021
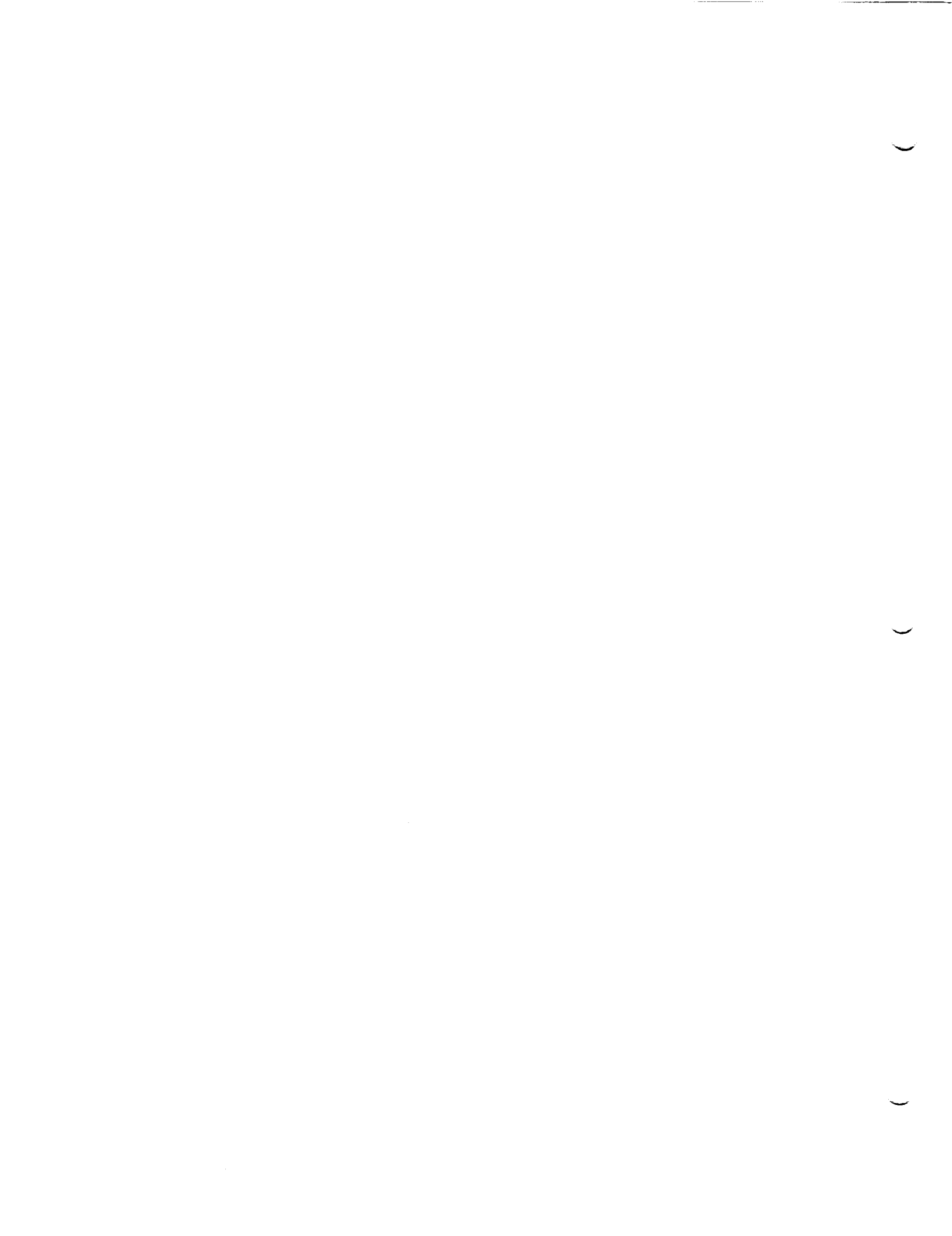
INVESTIGATION OF SSME ALTERNATE HIGH PRESSURE FUEL TURBOPUMP LIFT-OFF SEAL FLUID AND STRUCTURAL DYNAMIC INTERACTION

by

David A. Elrod
Assistant Professor
Mechanical Engineering Department
Virginia Polytechnic Institute and State University
Blacksburg, Virginia

ABSTRACT

The Space Shuttle Main Engine (SSME) alternate turbopump development program (ATD) high pressure fuel turbopump (HPFTP) design utilizes an innovative lift-off seal design that is located in close proximity to the turbine end bearing. Cooling flow exiting the bearing passes through the lift-off seal during steady state operation. The potential for fluid excitation of lift-off seal structural resonances is investigated. No fluid excitation of LOS resonances is predicted. However, if predicted LOS natural frequencies are significantly lowered by the presence of the coolant, pressure oscillations caused by synchronous whirl of the HPFTP rotor may excite a resonance.

ACKNOWLEDGEMENTS

NOMENCLATURE

A   cross-sectional area (L^2

a   diaphragm radius (L)

d_o jet diameter (L)

F   force (F)

f_r frequency ratio

h   diaphragm thickness (L)

L   jet developing flow region length (L)

$\dot{m}$ mass flow rate (M/T)

P   fluid pressure (F/L^2)

R   radius (L)

V   fluid velocity (L/T)

ρ fluid density (M/L^3)

ρ_d diaphragm density (M/L^3)

ϕ jet direction to surface normal angle

Subscripts

j   jet

r   radial

z   axial

0,1   zeroth- and first-order

INTRODUCTION

In the high pressure fuel turbopump (HPFTP) design of the Space Shuttle Main Engine (SSME) alternate turbopump development program (ATD), hydrogen from the discharge of the third stage pump impeller is used to cool the turbine-end roller bearing and turbine. Figure 1 is a cross-section of the ATD-HPFTP. Between the roller bearing and turbine, a lift-off seal (LOS) controls the coolant flow from the bearing discharge region to the turbine parts. Figure 2 shows details of the lift-off seal in the "closed" position. Before start-up, the corrugated LOS diaphragm holds the LOS seal element against a polished seal plate, preventing flow to the turbine. The chamber upstream of the LOS is fed by two sources: the roller bearing discharge flow and eight 3.5 mm (0.138 in.) diameter axial nozzles (see figure 2). When the turbopump is started, the increasing hydrogen pressure on the pump side of the LOS deflects the diaphragm axially until it seals on the LOS retainer. Coolant flows through radial holes in the seal element and diaphragm to cool the outer turbine elements, and past the seal element knife edge to cool the liners and rear face of the turbine disk.

A one dimensional analysis of the ATD-HPFTP coolant flow has been performed for 65% to 115% power levels (see Gregory, 1989). The structural dynamic character-istics of the LOS have been investigated by Brown (1989). In the present study, LOS fluid/structural interactions are investigated.
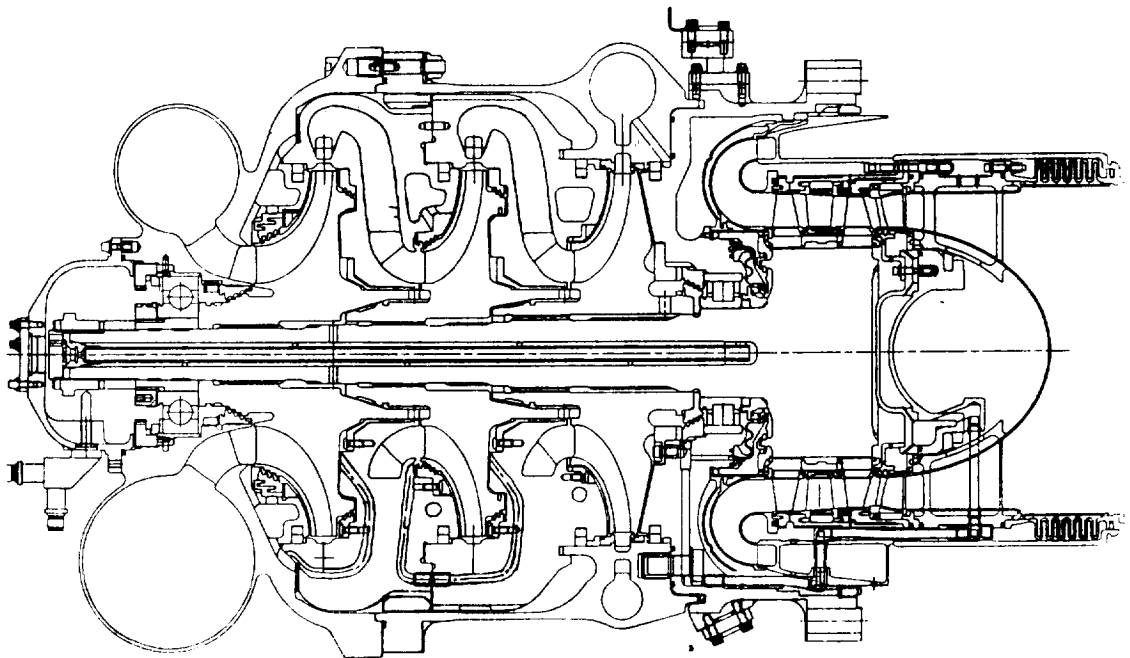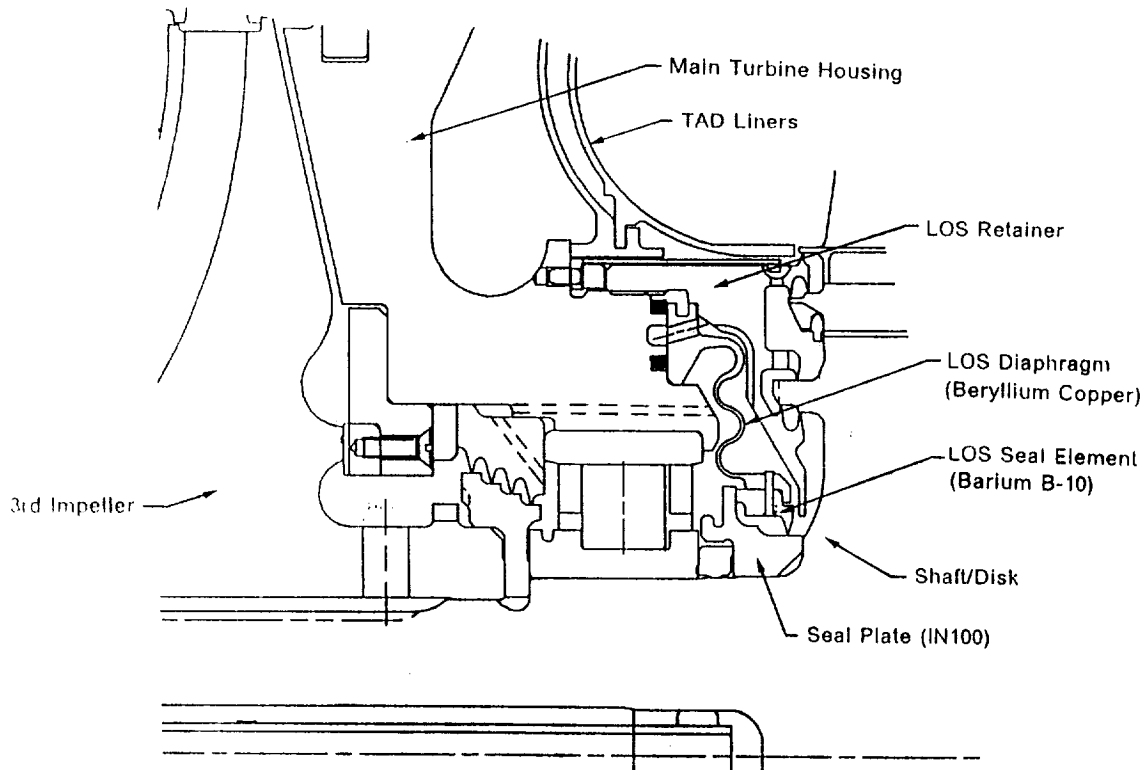

Figure 1. ATD-HPFTP cross-section.

X-1

Figure 2. ATD-HPFTP lift-off seal.

The following labels appear in the figure:
- Main Turbine Housing
- TAD Liners
- LOS Retainer
- LOS Diaphragm (Beryllium Copper)
- LOS Seal Element (Barium B-10)
- Shaft/Disk
- Seal Plate (IN100)
- 3rd Impeller

OBJECTIVES

The objective of the present work is to investigate the potential for fluid excitation of LOS structural resonances. Two questions which must be answered at the outset are:

(1) What are the predicted eigenvalues (natural frequencies) and mode shapes of the LOS structure?

(2) What are the coolant pressures and flow rates in the LOS region?

Question (1) is answered by Brown's analysis. His predictions are summarized in the next section. The flow rates and flow geometry provided by Pratt & Whitney (P&W), the ATD contractor, are then used to identify the most likely sources of excitation of LOS resonances. These sources are then analyzed individually.

LOS STRUCTURAL DYNAMICS

In a structural analysis of the LOS, the part of interest is the diaphragm/seal element assembly (see figure 2). The assembly has been modelled using NASTRAN, EAL (Engineering Analysis Language), and the P&W "Shell Deck" code. There are three mode "families" for this assembly: a ring family and two disk families. For a ring mode,

motion is radial, nodes are diametral, and waves are present along a circumferential line. For both disk mode families, motion is axial. A "diametral" disk mode has nodes along diametral lines, and waves along circumferential lines. A "circular" disk mode has concentric, circular nodes, and waves along radial lines.

Predicted natural frequencies of the diaphragm/seal element assembly are shown in figure 3. No circular disk modes are predicted below 20,000 Hz. The lowest predicted natural frequency is a diametral disk mode at 782 Hz, which is 29% higher than the ATD HPFTP 109% power level design speed of 606 Hz (36,353 rpm). Synchronous excitation of the diaphragm by the coolant will not excite a resonance. However, it should be noted that the natural frequency of a diaphragm depends on the fluid in which it is submerged. For a flat diaphragm, the ratio f_r of the natural frequency in a fluid of density ρ to the natural frequency in a vacuum is

$$f_r = \frac{1}{\sqrt{1 + \dfrac{0.669\,\rho a}{\rho_d h}}}$$

(Di Giovanni, 1982) where a is the diaphragm radius, h is the diaphragm thickness, and ρ_d is the density of the diaphragm material. The radius and thickness of the LOS corrugated diaphragm are approximately 86 mm (3.4 in.) and 0.8 mm (0.03 in.), respectively. The density of the diaphragm material is 8230 kg/m³ (514 lbm/ft³), and the coolant density is approximately 76 kg/m³ (4.7 lbm/ft³). A flat diaphragm with these dimensions in the LOS operating environment would have a frequency ratio of 0.78. For the corrugated diaphragm of the LOS, a frequency ratio of 0.78 would lower a 782 Hz natural frequency to 610 Hz - too near the 109% power level design speed.

ONE-DIMENSIONAL FLOW ANALYSIS

In this section, results of a P&W one-dimensional flow analysis are used to identify potential sources of seal-resonance excitation. In figure 4, the flow paths in the LOS region of the ATD-HPFTP are numbered. In the following discussion, they are referred to as resistances 1 through 6. The 115% power level flow predictions of P&W are listed in Table 1. Discussion of the fluid forces on the LOS are restricted to the 115% power level, for which pressure drops, fluid velocities, and, therefore, fluid forces, are highest.

Table 1. LOS Coolant Flow - 115% Power Level

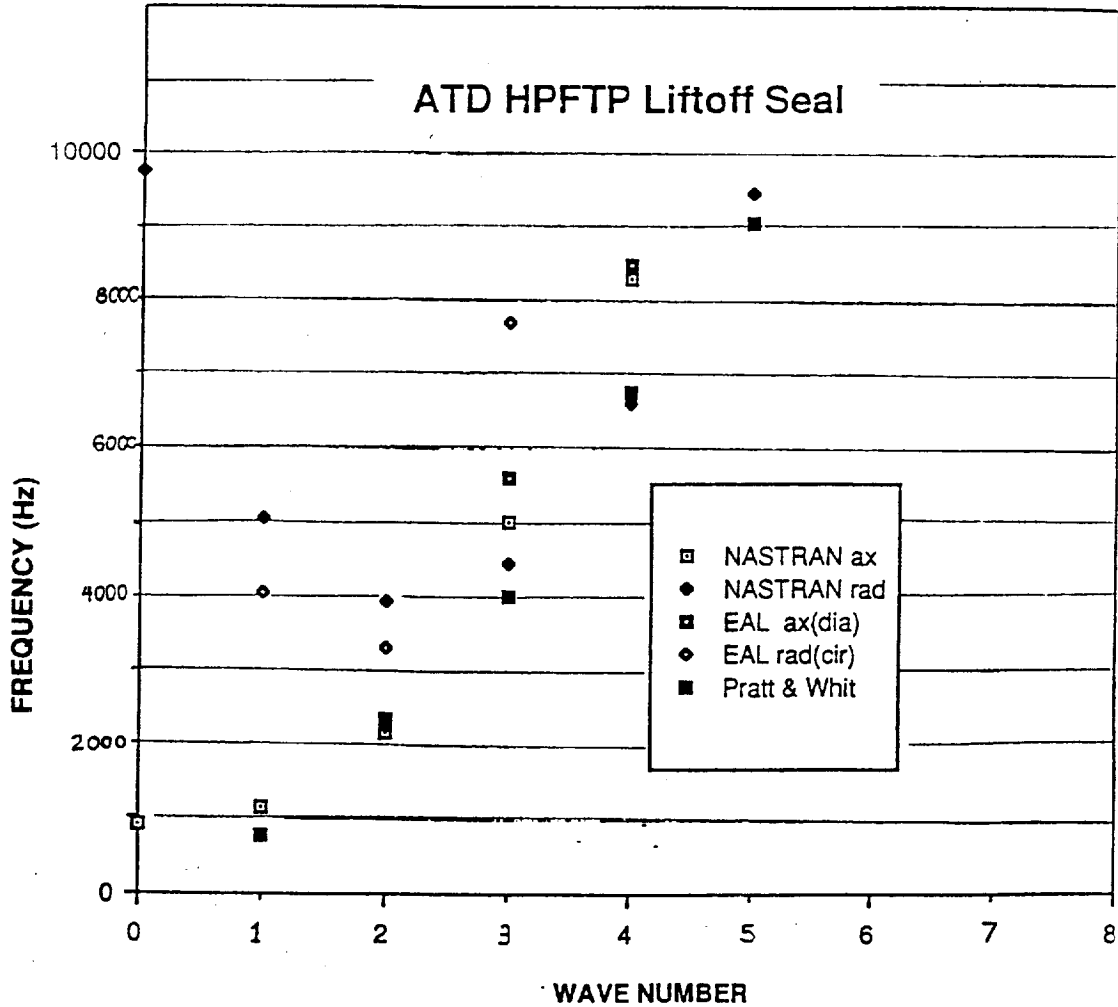| Resis. #	ΔP (bars)	$\dot{m}$ (kg/s)	ρ (kg/m³)	A (mm²)	V_z (m/s)	V_r (m/s)
1	29.8	1.207	76.4	77.	205.2	0.0
2	2.7	1.102	76.4	283.	50.1	0.0
3	5.4	2.309	76.2	366.	0.0	82.6
4	8.5	1.009	75.7	127.	0.0	105.0
5	71.5	1.300	76.2	52.	328.1	0.0
6	62.9	0.016	75.7	3.	0.0	70.5

Figure 3. LOS diaphragm/seal element natural frequencies.

For each restriction listed in Table 1, $\dot{m}$ is the mass flow rate, ρ is the density of the coolant at the restriction discharge, A is the cross-sectional area perpendicular to the assumed one-dimensional flow through the restriction, and V (= $\dot{m}/\rho A$) is the one-dimensional velocity. For restriction 1, A is the total cross-sectional area of eight 3.5 mm (0.138 in.) diameter nozzles. For restriction 2, A is the total cross-sectional area of fourteen passages through the roller bearing. Each of the fourteen passages is bounded by the inner diameter of the bearing cage, the inner race rail diameter, and two adjacent rollers (see figure 5). For restriction 4, A is the total cross-sectional area of sixteen 3.2 mm (0.125 in.) radial holes through the seal element and diaphragm. Though a one-dimensional analysis was used to model the coolant flow network, figure 4 and Table 1 indicate that flow through the LOS is highly three-dimensional.
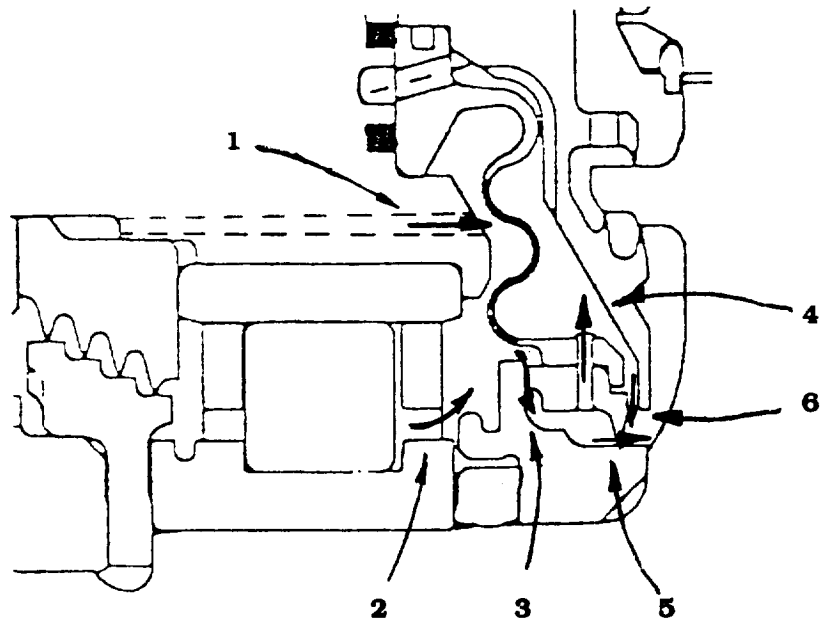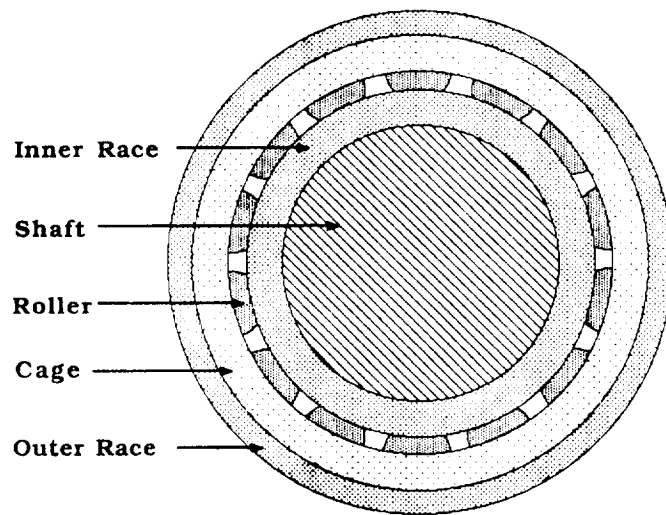
Figure 4. LOS coolant flow paths.

Figure 5. ATD-HPFTP roller bearing cross-section.

The predicted pressure drop across the corrugated diaphragm is the sum of the pressure drops across resistances 3 and 4. For the 115% power level, the diaphragm pressure drop is 13.9 bars (202 psi). The static axial force on the diaphragm/seal element assembly due to the diaphragm and restriction 5 pressure drops is greater than 20 kN (4500 lbf). Synchronous whirling of the HPFTP rotor (due to rotor unbalance) will cause flow oscillations at the rotor speed frequency in restrictions 3 through 6. The oscillations will produce dynamic forces, but at a frequency (606 Hz at the 109% power level) well below the predicted LOS resonances. The roller bearing coolant flow (restriction 2 in figure 4) may be roughly analyzed as 14 oblique jets discharging into a cross-flow, upstream of the LOS. However, the jets rotate at the bearing cage speed, which is less than half of the HPFTP rotor speed. Therefore, no excitation of LOS resonances by the bearing coolant flow is predicted.

Five of the six LOS flow paths shown in figure 4 have been eliminated as likely causes of LOS resonance excitation. The remainder of this study is an analysis of the fluid/structural interaction at the discharge of restriction 1 of figure 4. The factors which collectively point to a need for further analysis of this flow are:

(1) the high flow velocity through restriction 1,

(2) the distance from the nozzle exits to the LOS diaphragm (from 1.3 to 2.8 mm, according to P&W predictions); and

(3) the shape of the diaphragm corrugation at the point of jet impingement.

JET/DIAPHRAGM INTERACTION

In 1924, Wilfred Campbell explained a thin-turbine-disk, fluid excitation mechanism which he called "feathering". Campbell demonstrated experimentally that an axial flow of steam through the blades of a thin turbine disk could sustain a vibratory wave travelling opposite the direction of normal disk rotation. The wave was excited by striking the disk with a stick, and the amplitude of the sustained wave was a function of the flow rate of the steam. Campbell explained that, as turbine blades vibrate, the angles between the fluid flow and blade surfaces change, causing oscillating forces which support a "backward" traveling wave (see Campbell, 1924). In the ATD-HPFTP lift-off seal, the force of a jet impinging on the corrugated diaphragm surface depends on the angle between the surface and the jet flow direction. The angles between the axial jets exiting restriction 1 of figure 4 and the corrugated surface depend on the radial positions of the jets relative to the diaphragm. The question which must be answered is:

If a LOS resonance is momentarily excited (e.g., by start-up of the HPFTP), could flow from restriction 1 (figure 4) sustain the resonance vibration in a manner similar to the feathering action described by Campbell?

In the following paragraphs, the dissipation of the jet flow upstream of the LOS diaphragm is analyzed, and an equation is derived for the force on the diaphragm caused by a jet. Then, a perturbation analysis is applied to determine the force due to radial motion of the diaphragm.

Jet Flow - Upstream of the LOS diaphragm, circular jets emerge from eight 3.5 mm (0.138 inch) diameter nozzles. Figure 6 (from Rajaratnam, 1976) shows the characteristics of a circular jet flowing into a reservoir. A shear layer originates at the jet boundary as the jet comes out of the nozzle, penetrating into the jet and into the surrounding fluid as the jet flows away from the nozzle. Up to section 1-1 in figure 6,
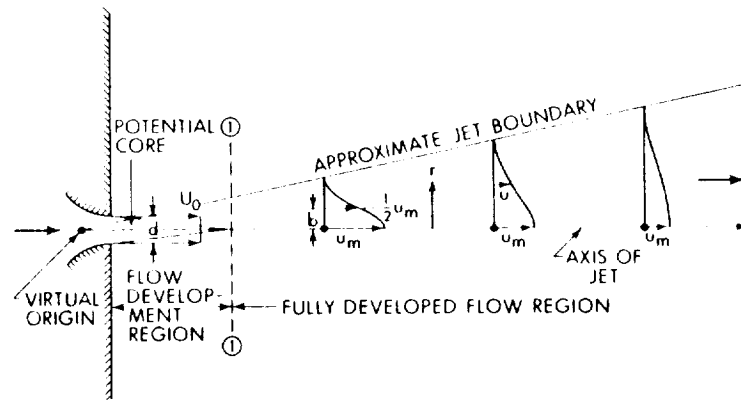
Figure 6. Definition sketch of circular turbulent jets.

there is a core of undiminished jet velocity. This region is called the "flow development region". Beyond section 1-1 in figure 6, in the "fully developed flow region", the centerline jet velocity decreases. The length of the flow development region is

$$L = 4.895 \, d_0 ,$$

where d_0 is the nozzle diameter. For the jets upstream of the LOS, L = 17.2 mm (0.676 in.). Since the clearance between the nozzles and the diaphragm is between 1.3 and 2.8 mm (0.051 and 0.110 in.), the full jet velocity impinges on the diaphragm.

Jet Force - The force on the diaphragm by each jet depends on the shape of the corrugation at the point of impingement. In figure 7, for a jet impinging on the surface shown at an angle ϕ from the surface normal, the force on the surface is approximately

$$F_j = \frac{1}{2}\rho\left(V_j\cos\phi\right)^2\frac{A_j}{\cos\phi} \tag{1}$$

where V_j is the jet velocity, and A_j (= $\pi d_0^2/4$) is the cross-sectional area of the jet. Figure 8 is a computer-generated detail drawing of the jet/diaphragm region. The figure was provided by P&W. The shaded region is a jet nozzle. The corrugation profile at the jet impingement location is approximately circular. In this analysis, ϕ is the angle shown in figure 8, at the location where the jet centerline intersects the corrugation profile. Dimensions of the diaphragm provided by P&W have been used to develop an equation for the angle ϕ as a function of the radial distance R from the diaphragm centerline to a point on the diaphragm in the jet region. When R is expressed in mm,

$$\phi = \tan^{-1}\left[\frac{74.6 - R}{\sqrt{3.6^2 - (R - 74.6)^2}}\right] \tag{2}$$

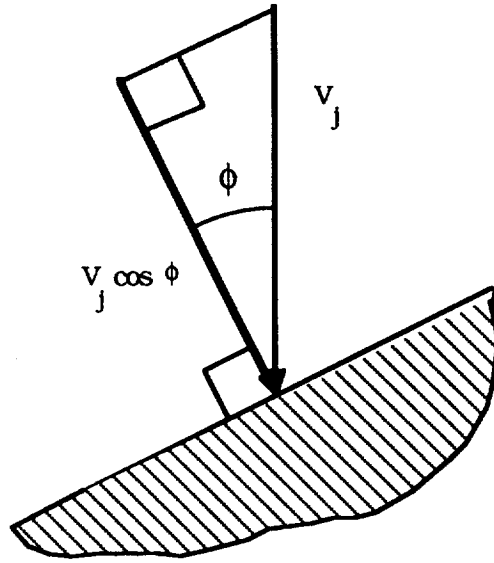From figure 8 and equation (1), the radial component F_{jr} of a jet force F_j is

X-7

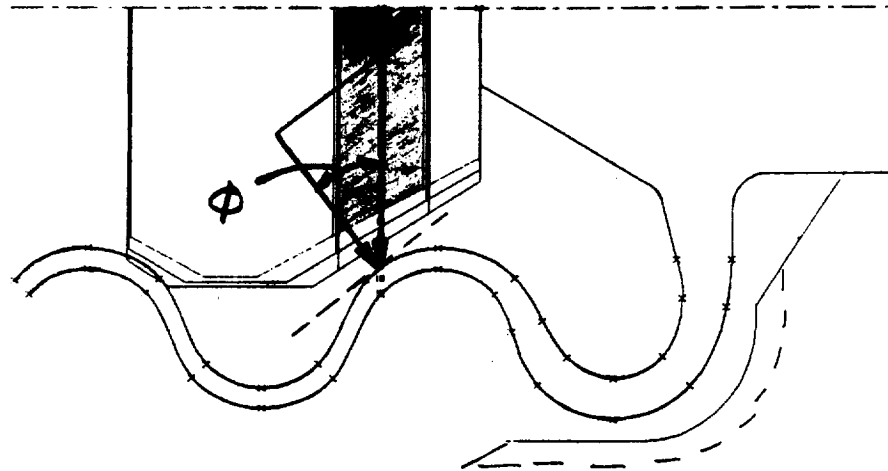Figure 7. Jet impinging on a surface at an angle ϕ.

Figure 8. Jet/diaphragm detail.

$$F_{jr} = \frac{1}{2}\rho V_j^2 A_j \cos\phi \sin\phi \qquad (3)$$

It is assumed that the eight jets strike the diaphragm concentrically, at a radius R. Relative motion between the diaphragm and jet nozzle locations causes a force perturbation if the angle ϕ changes with the motion. Motion of the diaphragm in the axial direction would cause no change in the angles between the jets and the diaphragm surface, and therefore no change in the jet forces on the diaphragm. If the diaphragm moves radially (and, therefore, the jets move radially relative to the diaphragm) the angle ϕ changes. The following perturbation analysis is used to approximate the change in radial force on the diaphragm caused by a small radial deflection of the diaphragm relative to the jet radial positions.

Jet Force Perturbation - To find the perturbation in the radial force F_{jr} on the diaphragm by jet j, due to small radial motion of the LOS diaphragm, equation (3) is expanded in terms of the perturbation variable

$$\phi_j = \phi_{j0} + \varepsilon\phi_{j1}$$

yielding

$$F_{jr1} = \frac{1}{2}\rho V_j^2 A_j \left[-\sin{}^2\phi_{j0} + \cos{}^2\phi_{j0} \right] \phi_{j1} \qquad (4)$$

where ϕ_{j1} is the perturbation of ϕ_j caused by radial motion R_{j1} of jet nozzle j relative to the diaphragm. Expansion of equation (2) in terms of the perturbation

$$R_j = R_{j0} + \varepsilon R_{j1}$$

yields the following equation for ϕ_{j1}:

$$\phi_{j1} = \cos{}^2\phi_{j0} \left\{ -\left[3.6^2 - \left(R_{j0} - 74.6 \right)^2 \right]^{-1/2} - \right.$$

$$\left. \left(R_{j0} - 74.6 \right)^2 \left[3.6^2 - \left(74.6 - R_{j0} \right)^2 \right]^{-3/2} \right\} R_{j1} \qquad (5)$$

To evaluate the perturbation F_{jr1} (equation (4)) caused by radial motion of the diaphragm, the nominal value ϕ_{j0} is calculated using equation (2) and the nominal radial position of jet impingement R_{j0}, and ϕ_{j1} is evaluated in terms of R_{j1}. Values of ρ and V_j are given in Table 1 for the 115% power level, and A_j is calculated using the known nozzle diameter, d_o. The following section provides the numerical results of this analysis.

NUMERICAL RESULTS

For each of the eight jets upstream of the LOS, $A_j = 9.6$ mm^2 (0.015 in^2). According to P&W drawings, the radius of the jet centerlines is 72.4 mm (2.85 in). Setting $R_{j0} = 72.4$ mm and using the density and velocity values in Table 1 for ρ and V_j, the following values are obtained from equations (2), (5), and (4):

$$\phi_{j0} = 0.66 \text{ rad} \quad (37.7\ )$$

$$\phi_{j1} = -.35\ R_{j1}$$

$$F_{jr1} = (-1.37 \text{ N/mm})\ R_{j1}\ .$$

The coefficient -1.37 N/mm in the expression for F_{jr1} may be interpreted as a radial stiffness introduced by a jet. The schematic in figure 9 provides a basis for explaining the effect of this radial stiffness.
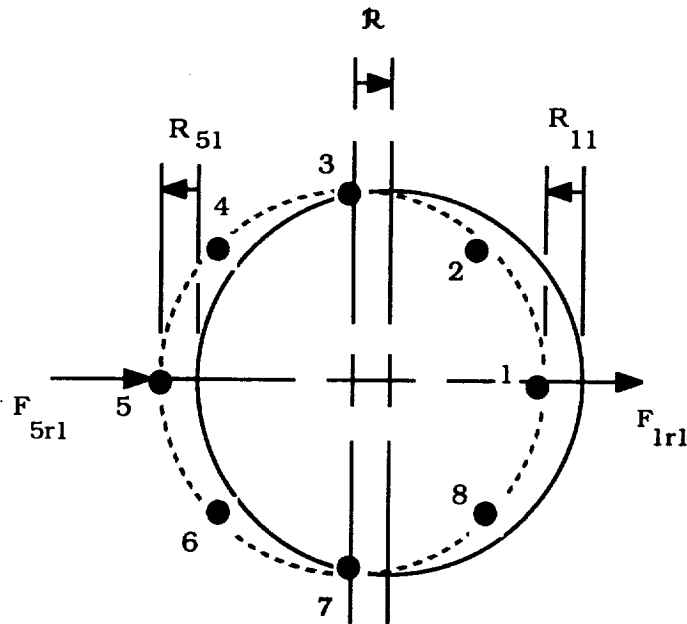

Figure 9. Relative motion of diaphragm and jet ring.

In figure 9, the black spots numbered 1 through 8 represent the eight jets upstream of the ATD-HPFTP lift-off seal. The circles represent a circle on the LOS diaphragm with the same diameter as the jet ring. If the diaphragm moves radially a distance $\mathfrak{R}$ relative to the jet ring, in the direction of jet number 1, the radial motion of jets 1 and 5 relative to the ring (R_{11} and R_{51}, respectively) are as shown. In this case, R_{11} is negative (towards the center of the diaphragm), and R_{51} is positive. The perturbation force on the diaphragm at jet 1 is F_{1r1} in the direction shown (positive radial direction). The perturbation force on the diaphragm at jet 5 is in the negative radial direction, as shown. Thus, the effect of the radial stiffness of the jets is to support radial motion of the diaphragm, or to reduce the radial stiffness, and therefore the ring mode natural frequencies. However, the magnitude of the jet radial stiffness has been calculated as 1.37 N/mm (8.8 lbf/in). The effect of this low radial stiffness on the LOS dynamic response is negligible.

CONCLUSIONS

The fluid/structural interactions of the ATD-HPFTP lift-off seal have been investigated for the possibility of fluid excitation of LOS resonances. The results of this study are summarized as follows:

- Synchronous pressure oscillations in the LOS region will not excite the resonances predicted by Brown and Pratt & Whitney, the ATD contractor. At the 109% power level, the synchronous force frequency is 77% of the lowest predicted natural frequency (782 Hz).

- Though the fourteen rotating jets exiting the roller bearing upstream of the LOS may produce oscillating loads on the LOS, the jets rotate at the bearing cage speed, less than half of the HPFTP operating speed, and a frequency well below the LOS natural frequencies.

- The eight axial jets upstream of the LOS affect the seal diaphragm as negative radial stiffnesses. However, the stiffness magnitudes are negligible compared to the material stiffness of the diaphragm/seal element assembly.

- For flat diaphragms, natural frequencies decrease as the density of the fluid in which the diaphragm is immersed is increased. If the natural frequencies of the corrugated diaphragm in the LOS are lowered significantly by the presence of the hydrogen coolant during operation of the ATD-HPFTP, synchronous pressure oscillations may excite LOS resonances.

REFERENCES

Brown, Andrew M., 1989, "Dynamic Modeling of Alternate Turbopump Liftoff Seal," internal NASA memorandum, June 22.

Campbell, Wilfred, 1924, "The Protection of Steam-Turbine Disk Wheels from Axial Vibration," *ASME Transactions*, No. 1920, pp. 31-160.

Di Giovanni, Mario, 1982, *Flat and Corrugated Diaphragm Design Handbook*, Marcel Decker, Inc., New York, NY, pp.196-197.

Gregory, H. K., 1989, V169 Flow and Bearing Load, computer printout, April 15.

Rajaratnam, N., 1976, *Turbulent Jets*, Elsevier Scientific Publishing Company, Amsterdam, The Netherlands, pg. 27.